Preparation and Characterization of Poly(Lactic Acid)-g-Maleic Anhydride + Starch Blends

Victor H. Orozco,[*1,2] *Witold Brostow,*[2] *Wunpen Chonkaew,*[2] *Betty L. López*[1]

Summary: Poly(lactic acid) (PLA) and starch copolymers are obtained by reactive blending - varying the starch compositions from 0 to 60%. PLA is functionalized with maleic anhydride (MA), obtaining PLA-g-MA copolymers using dicumyl peroxide as an initiator of grafting in order to improve the compatibility and interfacial adhesion between the constituents. PLA + starch blends without a compatibilizer do not have sufficient interfacial adhesion. Decomposition temperature of PLA is not affected by grafting. Glass transition temperatures and dynamic mechanical properties are affected since MA has a plasticizing effect. Along with an increasing starch content friction decreases while wear loss volume in pin-on-disk tribometry has a minimum at nominal 15% wt. starch but increases at higher starch concentrations. The residual depth in scratching and sliding wear testing has a maximum at 15% starch; there is a minimum of storage modulus E′ determined in dynamic mechanical testing at the same concentration. Microhardness results also reflect the plasticization by MA.

Keywords: blends; brittleness; dynamical mechanical analysis; grafting; polylactic acid; starch; tribological properties

Introduction

Poly(lactic acid) (PLA) exhibits high biodegradability; however, it is expensive – what limits its uses in disposable items. In order to maintain the PLA biodegradability and reduce the cost, some composites have been made incorporating dry starch into PLA matrix.[1–4] Due to the characteristics of starch, it can be used as filler producing an increase of the material rigidity and also an increase in intrinsic brittleness of the PLA, limiting the range of starch content.[5] The brittleness can be reduced by weakening the filler-filler interactions and at the same time reducing the glass transition temperature T_g. One uses for this purpose plasticizers such as water,[6] polyethylene glycol,[2] polypropylene glycol, ethyl and propyl citrates, glycerol[7] and sorbitol obtaining a thermoplastic starch (TPS) with ductility higher that neat starch. We note a discussion by Kopczynska and Ehrenstein[8] how important are interactions at interfaces for properties of multiphase materials.

TPS offers better material processability and better dispersion than neat PLA. The main disadvantages of TPS are its moisture sensitivity, limited temperature stability, plasticizer loss and starch recrystallization with time leading to embrittlement;[9,10] consequently the plasticizers provide desired results only at low concentrations. For instance the elongation at break is 5% higher for PLA + starch blends when polyols are used as plasticizers, this for any starch source.[5]

As already stated, mechanical properties such as tensile strength and elongation at break of composites depend on interfacial adhesion between the solid particulate

[1] Grupo Ciencia de los Materiales, Universidad de Antioquia, Calle 62 52 59 Medellín, Antioquia, Colombia
E-mail: victorhugo.orozco@gmail.com
[2] Laboratory of Advanced Polymers & Optimized Materials (LAPOM), Department of Materials Science and Engineering, University of North Texas, Denton, TX 76203-5310, USA

(filler) and the polymer matrix.[8] Thus, if matrix + filler interactions are not favored by thermodynamics, a chemical modification of the starch surface is called for. One way to compatibilize the starch is by grafting polymeric chains on the starch surface using a suitable catalyst,[11,12] which makes it miscible with the PLA matrix.

Due to their high reactivity and availability, difunctional molecules such as diisocyanates have been used as chemical connectors between starch and polymeric matrices in order to obtain a graft copolymer that can serve as a compatibilizer. Starch/graft/polycaprolactone (PCL) in small amounts has been used to compatibilize starch + PLA blends. There was improvement in the tensile strength; however, degradation products are harmful - what limits the use of PCL in agriculture and medicine. Anhydrides with unsaturated bonds have also been used in polymer compatibilization.[4,13] Composites containing 50% starch were also prepared, but only 10–20% of starch grafted to PLA[1] showed a significant tensile strength improvement.

Although grafting improves properties of starch-containing composites,[14] the grafting process generally requires elaborate experimental set-ups, expensive catalysts, relatively long reaction times, works in a limited temperature range[13] and needs a large quantity of solvent. It is necessary to purify the final products – a disadvantage for industrial production. Hence a more interesting compatibilization method consists in modifying the polymer matrix by grafting a polar group that can react with the starch.[3] Maleic anhydride (MA) has been grafted on polyolefin matrices;[15] the procedure is not complicated, performed using a free-radical initiator such as an organic peroxide. Organic peroxides have been used in a variety of applications[16–24] and these procedures can be used on a large scale.

In this work we have functionalized polylactic acid (PLA) with maleic anhydride (MA) (PLA-g-MA) using dicumyl peroxide as an initiator of the grafting process in order to improve compatibility and interfacial adhesion between the PLA and starch. Different amounts of starch have been used in the reactive blending. A variety of properties have been determined – including tribological ones which are important for the final application.[25]

Experimental Part

Materials

The PLA injection grade was supplied by Jamplast Inc., Ellisville, USA; the dycumyl peroxide, maleic anhydride and potato starch were purchased from Sigma Aldrich; chloroform and methanol were purchased from Merck, reagent grade.

Blend Preparation

The blends were prepared in a Brabender Type 6 mixer at 160 °C with the blade speed of 80 rpm. First, the PLA was molten inside the blender, second the dycumyl peroxide initiator was added and reacted for 5 minutes, then the grafting reaction with the maleic anhydride continued for another 5 minutes. At the end, the blending reaction with starch lasted 5 minutes. The polymer blends were chopped into small pieces and were heated up to 150 °C and kept there for 30 minutes after which the samples were compression moulded.

The MA compatibilized blends contained in turn 15, 25, 35, 50 and 60 wt. % starch. The following symbols are used in obvious notation: 15S/85(PLA-g-MA), 25S/75(PLA-g-MA), 35S/65(PLA-g-MA), 50S/50(PLA-g-MA), 60S/40(PLA-g-MA); 35S/65(PLA) represents a non-compatibilized blend used as a reference sample.

PLA is a clear and semi-transparent polymer. The blends are white even with a minimum amount of starch. Their macroscopic appearance is homogenous, suggesting that there is no phase separation.

Fourier Transform Infrared Analysis

A portion of blend was dissolved in 50 ml $CHCl_3$ under reflux and the solution was filtered. The $CHCl_3$ soluble fraction of the filtrate was precipitated with methanol and

the resulting product was extracted with 50 mL methanol in a Soxhlet for 24 hours, after which the polymeric material was dried at 60 °C. The FTIR spectra were recorded with a Perkin-Elmer Spectrum One spectrometer; powdered samples were evaluated with KBr pellet technique in transmission.

Scanning Electron Microscopy

A Scanning Electron Microscope (SEM) JEOL JSM-5800 at 25 keV was used to study the interfacial adhesion and the dispersion of starch in the PLA matrix. The specimens were broken in liquid nitrogen and the fracture surface sputtered with Au. The tracks generated by the pin-on-disc test were also measured by SEM.

Thermogravimetric Analysis

Thermo gravimetric analysis (TGA) was carried out with a TA Instruments Q500. Each sample was run from 25 to 700 °C at the heating rate of 10 °C/min under a nitrogen atmosphere. Then the temperature was increased to 800 °C using the same rate in air atmosphere. The TGA technique has been well explained by Menard[26] and also by Lucas and her colleagues.[27]

Modulated Differential Scanning Calorimetry

Modulated differential scanning calorimetry (MDSC), TA Instruments Q100 was used to determine glass transitions T_g, melting points T_m, crystallization temperatures T_c and melting enthalpies. The thermal history was erased during the first run at a high heating rate up to 190 °C followed by a fast cooling to −50 °C. Then the heating rate was modulated ±1 °C/min minute with a ramp 2 °C/min to 200 °C. DSC is also explained by Menard[26] and by Lucas and her coworkers.[27]

Dynamical Mechanical Analysis (DMA)

The storage modulus E′, loss modulus E″ and mechanical damping tangent (tan δ) were measured using Perkin Elmer DMA-7 machine. Physical significance of these parameters is explained by Menard[26,28] and by Lucas and her colleagues.[27] Specimens of rectangular shape (length: 1.8 cm, width: 0.6 cm, thickness: 0.2 cm) were analyzed in the 3-point bending mode at 1.0 Hz in dry nitrogen (20 mL/min) from 20 °C to 120 °C using the heating rate of 5 °C/min.

Pin-on-disk Tribology

Pin-on-disc tests were made in an Implant Science ISC-200PC tribometer at a constant load against a stainless steel indenter at 21 °C; the wear track radius R = 5.0 mm; pin end spherical radius r = 0.3 mm, normal load 2.0 N, linear speed 98 mm/s, and distance 500 m.

ImageJ® public domain software developed by Wayne Rasband was used to measure the tracks width. Volume loss was calculated as.[29]

$$V = 2\pi R\left(r^2 \sin^{-1}\frac{d}{2r} - \left(\frac{d}{4}\right)(4r^2 - d^2)^{1/2}\right) \quad (1)$$

Here d is the wear track width (an average of 20 determinations).

Scratch Testing

The tests were carried out using a CSEM Micro-Scratch Tester (MST) using a procedure described before.[30–32] Sliding wear was determined by performing 15 scratch runs along the same groove[33,34] at the constant normal load 5.0 N, scratch length 5.0 mm, scratch velocity 5.26 mm/min at room temperature. Moreover, progressive increasing load scratch tests were made from the initial load of 0.03 up to 30.0 N; the loading rate was 10.0 N/minute, the scratch velocity 1.67 mm/minute and the scratch length again 5.0 mm. A 200 μm diameter conical diamond indenter was used in all tests. The results include the instantaneous penetration depth R_p and the healing or residual depth R_h. The results reported are averages from several locations on a given sample. The viscoelastic recovery φ was calculated[30,31] as

$$\phi = 1 - R_h/R_p \quad (2)$$

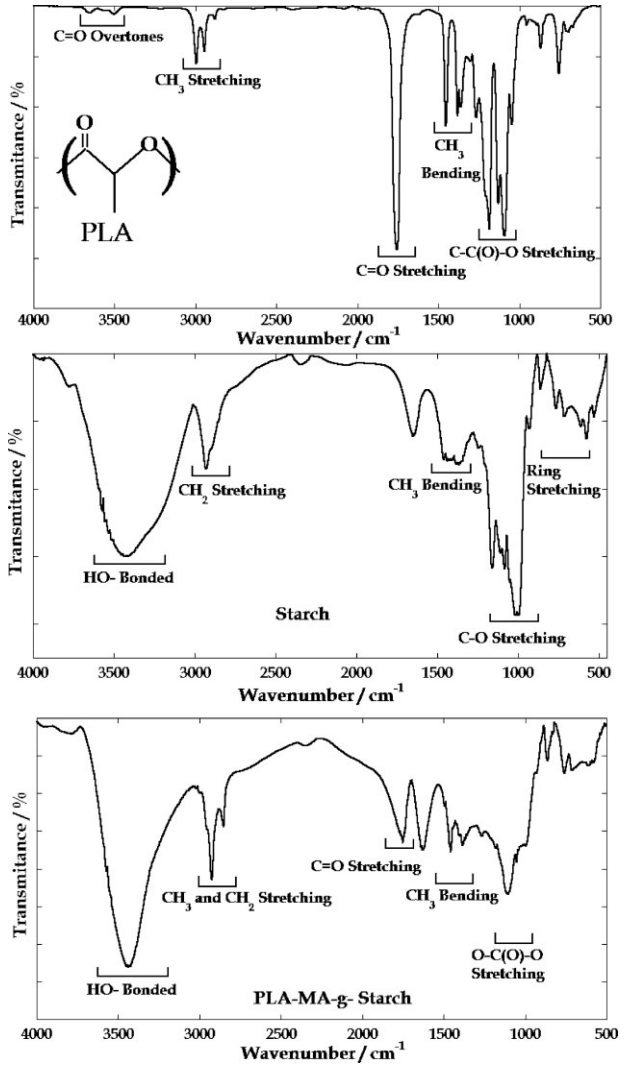

Figure 1.
FTIR spectra: a) PLA, b) starch and c) PLA-g-MA + starch.

Microhardness

Surface Vickers hardness H_v values were determined on a Shimadzu Microhardness HMV 2000 tester with a diamond pyramidal indenter and an optical microscope as

$$H_v = 1.8544P/D^2 \quad (3)$$

this machine leave a diamond pyramidal shape impression - whose diagonals length D is measured by using a micrometer eyepiece; the load P was 100 N applied for 15 s in each trial. Averages of a minimum of 15 readings are reported.

Infrared Analysis Results

Figure 1 shows IR-spectra of PLA, starch and the extracted polymer. The PLA spectrum shows C=O stretching overtones at 3660–3500 cm^{-1} and CH_3 stretching at

3000–2940 cm^{-1}. The C=O cm^{-1} stretching at 1761 cm^{-1} and the O–C=O stretching at 1190–1090 cm^{-1} are characteristics of ester bonds. The starch spectrum shows distinctive peaks and bands for carbohydrates: a broad band in the range of 3760–3010 cm^{-1} indicates hydrogen bonded hydroxyl groups, CH_2 stretching at 2932 cm^{-1}, O–C stretching in the range of 1180–960 cm^{-1}, and anhydroglucose ring stretching vibrations in the range 861–575 cm^{-1}. Since maleic anhydride homopolymer and unreacted starch were removed during extraction of the blends, the spectrum of extracted polymer corresponds only to the starch/PLA-g-MA copolymer. This spectrum shows a combination of PLA and starch peaks. Since the amount of maleic anhydride (1% with respect to PLA) present in the blends is small, the C=O stretching of maleic acid or anhydride peak is very weak and might be overlapping with the carbonyl band of PLA. Possibly the extent of grafting is too low and IR spectroscopy is not a technique sensitive enough to identify these changes.

Morphological Analysis

SEM micrographs of 35S/65(PLA) and 35S/65(PLA-g-MA) blends are shown in Figure 2. Figure 2a for non-compatibilized blend shows two phases, the PLA matrix and starch grains. There are also holes and cavities at the interface between both phases. The holes are formed during the fracture procedure in the sample preparation. The track smoothness indicates that starch grains are easily removed. The cavities and holes prove very poor interfacial adhesion due to the hydrophobic character of PLA while starch is highly hydrophilic. This is the reason for thermodynamic incompatibility that cannot be overcome by simple blending.[3]

The compatibilized blend (Figure 2b) shows a different morphology. Now starch grains are still covered by strongly adhesive PLA. The fracture surface exhibits high roughness while the cracks go randomly through the matrix avoiding starch grains. The interphase between the PLA and starch is stable and does not show stress fracture.

Figure 3 shows compatibilized blends with the lowest 15S/85(PLA-g-MA) – Figure 3a – and the highest 60S/40(PLA-g-MA) starch content– Figure 3b –, respectively. Figure 3a shows still two phases but does not show cavities, only occasionally a crevice around a starch granule. Holes where starch particles were removed such as in Figure 2a are not observed. Instead, the starch phase is broken along with the matrix-starch interphase. There is a compatibilization. Even in blends with the highest starch content the starch grains are completely covered by PLA.

All compatibilized blends show better interaction between PLA and starch. Chemical interactions might result from a transesterification reaction among starch hydroxyl groups, grafted acid hydroxyl groups or anhydride groups on PLA. Physical interaction is possible through hydrogen bonds.

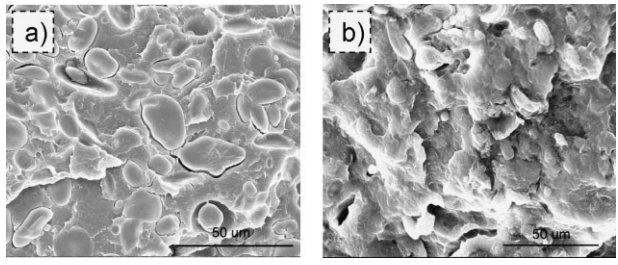

Figure 2.
SEM micrographs: a) PLA + starch blends without maleic anhydride (35S/65(PLA)); b) PLA-g-MA + Starch (35S/65(PLA-g-MA)).

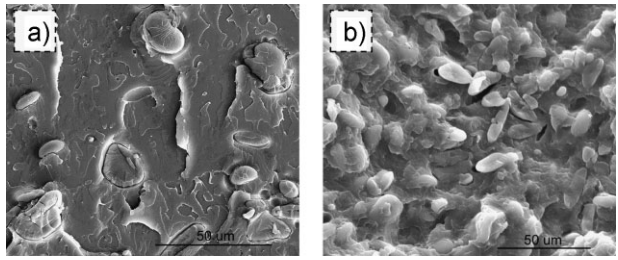

Figure 3.
SEM micrographs PLA-g-MA + starch blends: a) 15S/85(PLA-g-MA), b) 60S/40(PLA-g-MA).

The blending conditions allow homopolymerization of maleic anhydride via a side reaction producing low-molecular weight polymers that can act as plasticizers and decrease the interfacial energy between the two phases and improve the wetting of the starch with molten matrix material. Given these results, we expect better properties in compatibilized blends.

Thermogravimetric Analysis

Table 1 summarizes the results for all blends; Figure 4 presents a typical TGA diagram. Three weight-loss processes can be observed: the first is due to loss of water and is about the same for all blends; then decomposition of starch, finally thermal decomposition of PLA. For all samples during pyrolysis in an inert gas atmosphere char formation is observed. Changing to an oxygen atmosphere and increasing the temperature up to 800 °C results in a complete oxidization of the residue with CO_2 as the final product.

We see that Table 1 shows that the maximum temperature for starch and PLA decomposition in all blends (compatibilized or otherwise) does not change significantly. Thus, the blend thermal stability is little affected by PLA modification and reactive blending.

The char formation increases along with the starch content increase. Thus, surface interactions between starch and the matrix protect the blend to some extend from thermal degradation below 700 °C.

Modulated Differential Scanning Calorimetry Results

Physical significance of glass transitions has been discussed before.[26–28,35,36] All blends show the same thermal transitions. Figure 5 shows a typical reversible and non-reversible calorimetric process of the MDSC run for the sample 35S/65(PLA-g-MA). Four reversible thermal events are observed: the glass transition T_g of the PLA matrix, a broad and weak exothermic peak as a crystal phase transition of the PLA and two endothermic peaks for melting of two distinct PLA crystalline phases. Irreversible thermal events also present four transitions:

Table 1.
Thermal Transitions of PLA + starch blends.

Sample	T_{d1}/°C	T_{d2}/°C	PLA/%	starch/%	char/%
Starch	312	–	0	96.0	4.0
PLA-g-MA	–	369	100.0	0	0
15S/85(PLA-g-MA)	307	367	86.7	11.5	1.9
25S/75(PLA-g-MA)	323	370	77.9	19.1	3.0
35S/75(PLA-g-MA)	308	369	68.8	26.3	4.9
50S/50(PLA-g-MA)	309	369	36.7	56.2	6.1
60S/40(PLA-g-MA)	312	368	48.8	43.6	7.7
35S/65PLA	316	371	68.7	26.7	4.6

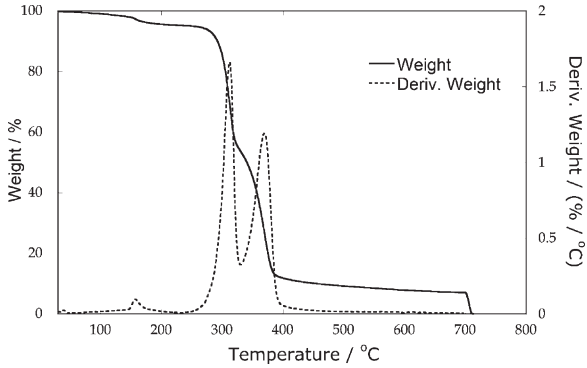

Figure 4.
A typical TGA diagram; the sample is 60S/40(PLA-g-MA).

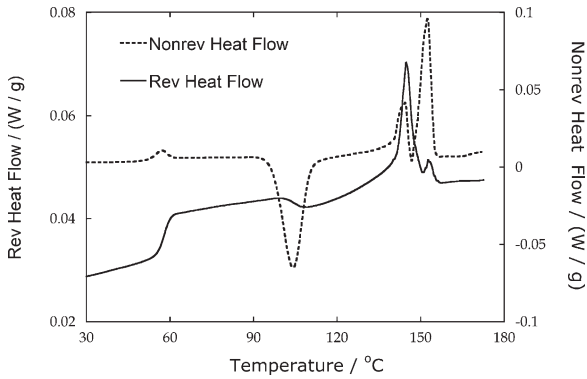

Figure 5.
A typical MDSC run for a PLA + starch sample: 35S/65(PLA-g-MA).

an endothermic peak associated with stress relaxation because the macromolecules are frozen in the glassy state in a non-favourable conformation; a sharp exothermic peak above T_g which is attributed to cold crystallization of PLA; finally, in two endothermic peaks due to transesterification reaction.[37]

Table 2 summarizes the MDSC thermal transition for all blends. Figure 6 shows both T_g and enthalpy of melting H_m as a function of the starch content. For blends with starch content greater than 15%, T_g increases and then nearly reaches a steady value at 58 °C. The increase can be explained by starch hindering movements of PLA chains.

The sample 15S/85(PLA-g-MA) shows the lowest T_g and the highest H_m. Apparently the low starch content increases the probability of homopolymerization of MA - leading to a low molar mass plasticizer that lowers T_g and facilitates crystallization of PLA; see Jacobsen and Fritz.[2] However, the degree of crystallinity is unaffected since H_m remains constant.

Table 2.
Thermal Transitions of PLA + starch blends.

Sample	T_g/°C	T_c/°C)	H_m/(J/g)*	T_m/°C)
PLA	58	108	1.71	147–153
PLA-g-MA	57	107	1.66	146–153
15S/85(PLA-g-MA)	56	101	13.02	144
25S/75(PLA-g-MA)	58	109	5.49	146–154
35S/65(PLA-g-MA)	58	104	3.62	145
50S/50(PLA-g-MA)	58	107	1.12	146
60S/40(PLA-g-MA)	58	100	1.10	145–154
35S/65PLA	58	110	0.90	148–1523

*Relative to PLA content.

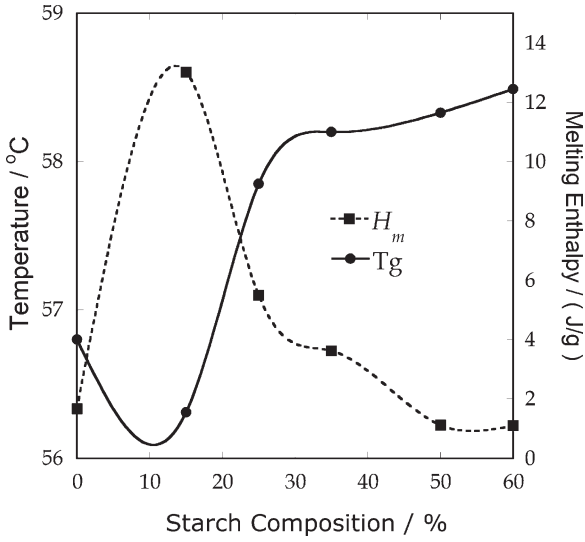

Figure 6.
Glass transition temperatures and enthalpies of melting vs. starch content.

Dynamic Mechanical Analysis Results

Figure 7 presents a DMA thermogram for 35S/65(PLA-g-MA). Figure 7a shows storage modulus E′ and loss modulus E″ vs. temperature diagrams. Two transitions are observed. The first one at ≈60 °C is the glass transition of PLA matrix. The second one at ≈110 °C reflects cold crystallization of the PLA.

Table 3 summarizes T_g results obtained from peaks of E″(T). The values are similar to those obtained by MDSC. The fact that different techniques do not provide identical T_g values has been discussed before.[26–28,35,36]

Figure 7b shows the storage modulus E′ vs. starch content. As in MDSC results, the storage modulus increases with starch content because the stiffness of the blends increases.[5] The lowest value of E′ is found

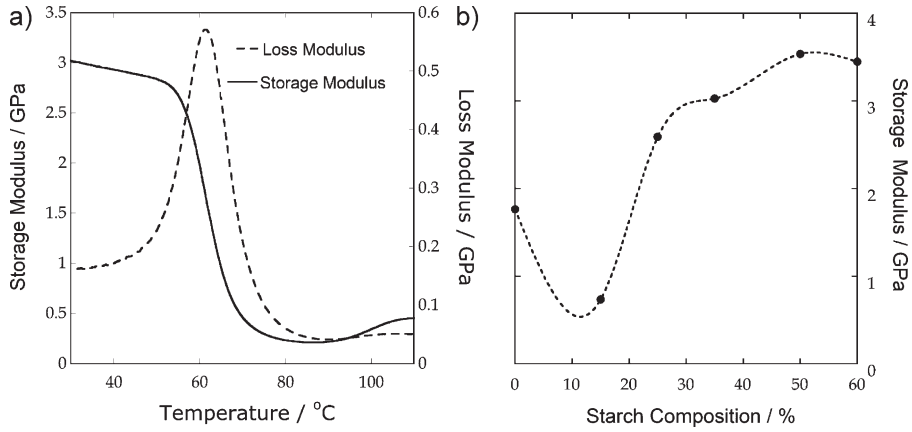

Figure 7.
a) DMA thermogram for 35S/65(PLA-g-MA) with storage and loss modulus vs. temperature; b) storage modulus vs. starch content at 30 °C

Table 3.
Thermal Transitions of PLA + starch composites from E″ peaks of DMA.

Sample	T_g/°C
PLA	62
PLA-g-MA	59
15S/85(PLA-g-MA)	61
25S/75(PLA-g-MA)	61
35S/75(PLA-g-MA)	62
50S/50(PLA-g-MA)	63
60S/40(PLA-g-MA)	61
35S/65PLA	65

for 15S/85(PLA-g-MA); this is again the plasticizer effect already discussed in Section 6 above.

Tribology Results

Service performance of polymeric components depends naturally on their tribological properties – as reviewed in.[31] We begin with results of wear and dynamic friction obtained using a pin-on-disk tribometer.

Figure 8 shows friction variations vs. starch content. A decrease of the dynamic friction is seen as the starch content increases - indicating self-lubricating by starch. Starch particles have a uniform size - seen above in SEM micrographs (Figure 3b). Since there are no friction studies on starch that we know of, it would be interesting in the future to study starch containing blends with different matrices.

Figure 9 presents 50S/50(PLA-g-MA) micrographs: (a) the wear track and (b) a zoom of the wear track. We see a good dispersion of starch particles in the track. The particles peel off the PLA surface – confirming our explanation above that they diminish the friction.

Figure 10 presents the wear volume calculated from[29] Eq. (1) and wear factor vs. starch content. Wear factor is the volume loss per distance at a given load (mm^3/Nm). Although the friction decreases with starch content, the volume loss increases. The maximum volume loss value is for the sample with 60% starch content. 15S/85(PLA-g-MA) exhibits the lowest volume loss because the plasticization effect of the maleic anhydride homopolymer.

We now discuss results of sliding wear determination by multiple scratch tests along the same groove.[2,33,38–40] Figure 11a presents results for a blend with 25% of starch content. Samples with starch

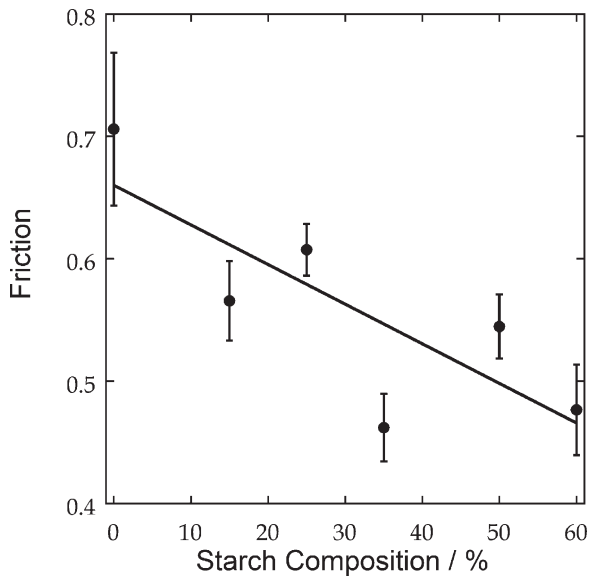

Figure 8.
Friction variations vs. starch content of the blends.

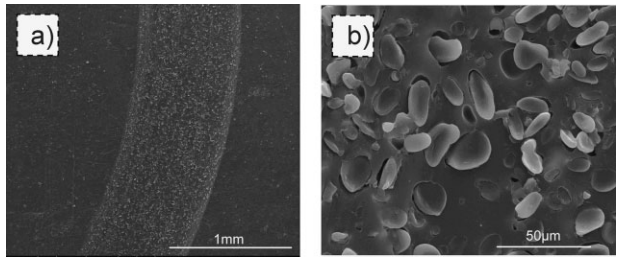

Figure 9.
50S/50(PLA-g-MA) micrographs: (a) the wear track and (b) a zoom of the wear track.

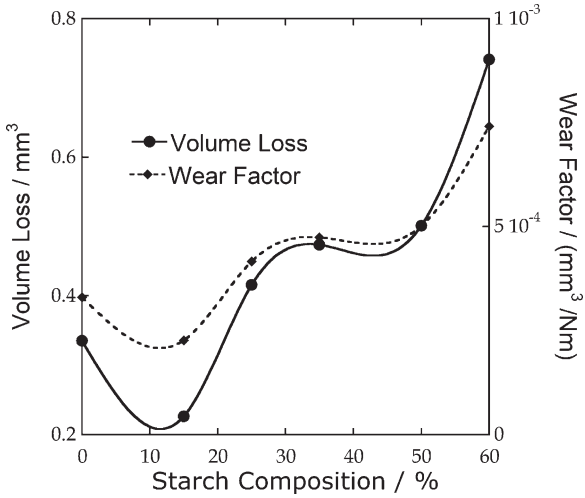

Figure 10.
Wear volume and wear factor variation vs. starch content of the blends at 22 °C.

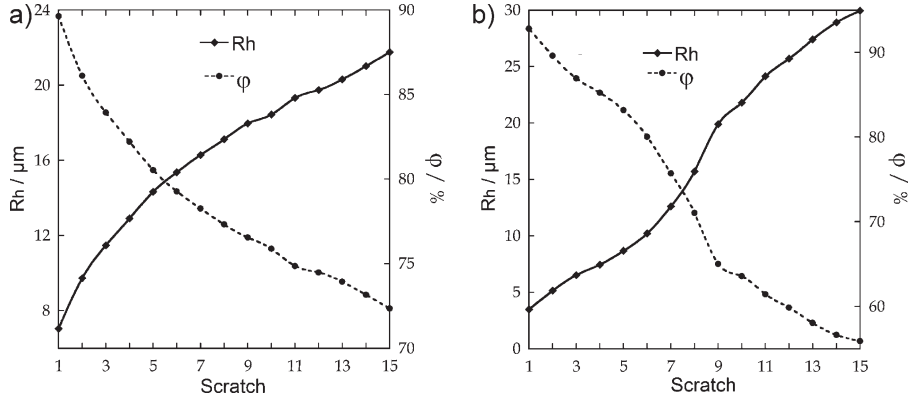

Figure 11.
Blends scratching behaviour: a) starch content 25 wt. %; b) starch content 60%.

concentration between 25 and 60% have the same trend but are not included for brevity. Figure 11b for the blend with highest starch content, 60S/40(PLA-g-MA), shows relatively small R_h variations until seventh scratch and larger changes afterwards. We recall that for polystyrene there is no strain hardening[39,40] – a fact

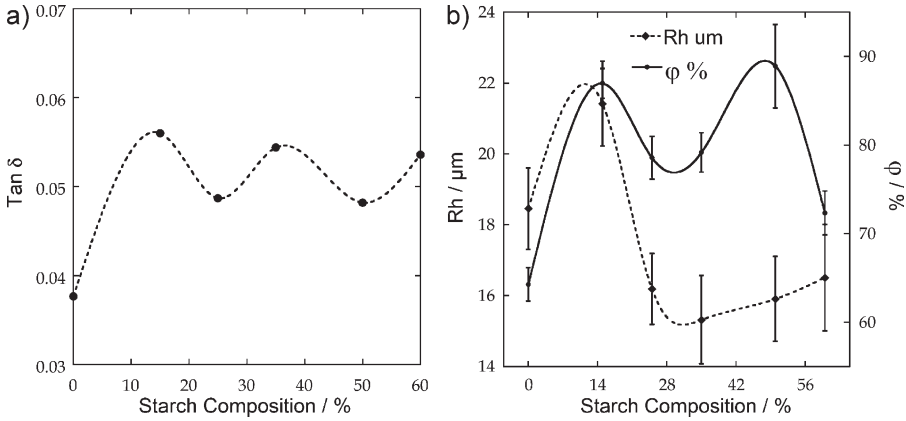

Figure 12.
a) tan δ vs. starch content; b) healing depth R_h and the viscoelastic recovery φ vs. starch content.

which contributed to formulating a definition of brittleness.[34] In the materials now investigated we do not see strain hardening either.

Figure 12a shows healing depths R_p and the viscoelastic recovery φ calculated from Eq. (2) obtained after 15 scratches vs. starch content in the blends. We see two maxima, namely at 15S/85(PLA-g-MA) and 50S/50(PLA-g-MA) for both R_p and φ. Thus, these samples have lower scratch resistance than the other ones but high viscoelastic recovery.

We have demonstrated[41] the existence of a relationship between the penetration depth R_p and tan δ, thus between a tribological and a dynamic mechanical property. Since tan $\delta = E''/E'$, low tan δ values reflect solid-like behaviour while high tan δ indicates liquid-like behaviour.[41] Figure 12b shows tan δ vs. starch content. Going from the left that is from the polymer without starch, we see first an increase of tan δ. This is the plasticizing effect of MA already pointed out before. The consecutive minima and maxima in Figure 12b are also reflective of maxima and minima in Figure 12a. Because of plasticization, 15S/85(PLA-g-MA) has the deepest R_p but the highest healing depth R_h; a softer material can be penetrated more but also recovers more. The softness is also the reason why the volume loss in Figure 10 is the lowest.

Microhardness

A softer material is expected to have a deeper scratch groove. Nanoindentation studies show that inside of a scratch groove the nanoindentation is shallower than outside, an effect of densification.[42] The total cross-section area of the scratch groove has been related to the Vickers hardness.[43] For these reasons we have now performed microhardness determinations. The results are shown in Figure 13 as a function of the starch content.

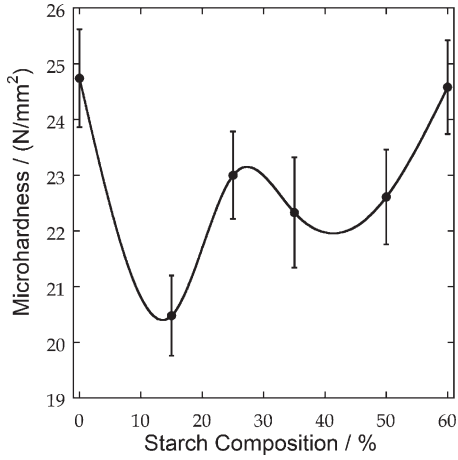

Figure 13.
Microhardness for PLA + starch samples vs. composition.

Let us compare the present results with those above, in Figure 10 and 11 in particular. Figure 13 confirms our earlier explanation in terms of plasticizing effect, resulting in softness, deeper grooves in scratching, more viscoelastic recovery and higher tan δ.

Acknowledgements: Partial financial support for this work was provided by the Robert A. Welch Foundation, Houston (Grant # B-1203) and also by the Hispanic and Global Studies Initiatives Fund (HGSIF) of the University of North Texas. We are also grateful to COLCIENCIAS and the Universidad de Antioquia, Colombia, for the financial support. The authors thank to the Colciencias Program "*Apoyo a la comunidad científica nacional a través de doctorados nacionales 2005*".

[1] L. Chen, X. Qiu, Z. Xie, Z. Hong, J. Sun, X. Chen, X. Jing, *Carbohydr. Polym.* **2006**, *65*, 75.
[2] S. Jacobsen, H. G. Fritz, *Polym. Eng. Sci.* **1996**, *36*, 2799.
[3] S. Kalambur, S. S. H. Rizvi, *J. Plast. Film Sheeting.* *200622*, 39.
[4] J. F. Zhang, X. Sun, *Biomacromolecules.* **2004**, *5*, 1446.
[5] T. Ke, S. X. Sun, P. Seib, *J. Appl. Polym. Sci.* **2003**, *89*, 3639.
[6] T. Ke, X. Sun, *J. Appl. Polym. Sci.* **2001**, *81*, 3069.
[7] M. A. Huneault, H. Li, *Polymer.* **2007**, *48*, 270.
[8] A. Kopczynska, G. W. Ehrenstein, *J. Mater. Ed.* **2007**, *29*, 325.
[9] O. Martin, L. Averous, *Polymer.* **2001**, *42*, 6209.
[10] N. Wang, J. Yu, P. R. Chang, X. Ma, *Carbohydr. Polym.* **2008**, *71*, 109.
[11] R. Mani, J. Tang, M. Bhattacharya, *Macromol. Rapid Commun.* **1998**, *19*, 283.
[12] D. Rutot-Houzé, P. Degée, R. Gouttebaron, M. Hecq, R. Narayan, P. Dubois, *Polymer Internat.* **2004**, *53*, 656.
[13] V. D. Miladinov, M. A. Hanna, *Ind. Crops Prod.* **2000**, *11*, 51.
[14] F. Xie, L. Yu, H. Liu, L. Chen, *Starch - Stärke.* **2006**, *58*, 131.
[15] F. J. Rodriguez-Gonzalez, B. A. Ramsay, B. D. Favis, *Polymer.* **2003**, *44*, 1517.
[16] L. Bazyliak, M. Bratychak, W. Brostow, *Mater. Res. Innovat.* **1999**, *3*, 132.
[17] L. Bazyliak, M. Bratychak, W. Brostow, *Mater. Res. Innovat.* **2000**, *3*, 218.
[18] M. Bratychak, L. Bazyliak, W. Brostow, O. Hevus, R. Fleiczuk, *Dopovidy Nacion. Akad. Nauk Ukrany* **2000**, *59*, 185.
[19] M. Bratychak, M. Bratychak, W. Brostow, O. Shyshchak, *Mater. Res. Innovat.* **2002**, *6*, 24.
[20] M. Bratychak, W. Brostow, *Polym. Eng. Sci.* **1999**, *39*, 1541.
[21] M. Bratychak, W. Brostow, V. Castaño, V. Donchak, H. Gargai, *Mater. Res. Innovat.* **2002**, *6*, 153.
[22] M. Bratychak, W. Brostow, V. Donchak, *Mater. Res. Innovat.* **2002**, *5*, 250.
[23] M. Bratychak, W. Brostow, O. Grynyshyn, O. Shyshchak, *Mater. Res. Innovat.* **2003**, *7*, 167.
[24] O. Zaichenko, M. Bratychak, W. Brostow, N. Mitina, O. Bednarska, *Rep. Natl. Acad. Sci. Ukraine* **2003**, *62*, 134.
[25] S. Karan, S. P. S. Gupta, *Mater. Sci. Eng., A.* **2005**, *398*, 198.
[26] W. Brostow, *Chapter 8* in: *Performance of Plastics*, Hanser/Gardner Publications, Munich-Cincinnati **2000**, p. 682.
[27] E. F. Lucas, B. G. Soares, E. Ed. C. Monteiro, *Caracterização de Polímeros*, e-Papers, Rio de Janeiro, **2001**, p. 366.
[28] K. P. Menard, "*Dynamic mechanical analysis*", CRC Press, Boca Raton, FL **2008**.
[29] M. D. Bermúdez, F. J. Carrión-Vilches, G. Martínez-Nicolás, *J. Appl. Polym. Sci.* **1999**, *74*, 831.
[30] W. Brostow, B. Bujard, P. Cassidy, H. Hagg, P. Montemartini, *Mater. Res. Innovat.* **2002**, *6*, 7.
[31] W. Brostow, J.-L. Deborde, M. Jaklewicz, P. Olszynski, *J. Mater. Ed.* **2003**, *25*, 119.
[32] W. Brostow, M. Jaklewicz, *J. Mater. Res.* **2004**, *19*, 1038.
[33] W. Brostow, G. Darmarla, J. Howe, D. Pietkiewicz, *e-Polymers.* **2004**, 025.
[34] W. Brostow, H. E. Hagg Lobland, M. Narkis, *J. Mater. Res.* **2006**, *21*, 2422.
[35] W. Brostow, R. Chiu, I. M. Kalogeras, A. Vassilikou-Dova, *Mater. Lett.* **2008**, *62*, 3152.
[36] W. Brostow, S. Deshpande, D. Pietkiewicz, S. R. Wisner, *preprint* **2008**, University of North Texas, Denton.
[37] V. H. Orozco, A. F. Vargas, B. L. López, *Macromol. Symp.* **2007**, *258*, 45.
[38] M. D. Bermúdez, W. Brostow, F. J. Carrión-Vilches, J. J. Cervantes, G. Damarla, J. M. Perez, *e-Polymers.* **2005**, 003.
[39] M. D. Bermudez, W. Brostow, F. J. Carrion-Vilches, J. J. Cervantes, D. Pietkiewicz, *Polymer.* **2005**, *46*, 347.
[40] M. D. Bermúdez, W. Brostow, F. J. Carrión-Vilches, J. J. Cervantes, D. Pietkiewicz, *e-Polymers* **2005**, 001.
[41] W. Brostow, W. Chonkaew, K. P. Menard, *Mater. Res. Innovat.* **2006**, *10*, 389.
[42] B. D. Beake, G. A. Bell, W. Brostow, W. Chonkaew, *Polym. Int.* **2007**, *56*, 773.
[43] W. Brostow, W. Chonkaew, L. Rapoport, Y. Soifer, A. Verdyan, *J. Mater. Res.* **2007**, *22*, 2483.

